ChemComm

RSC Publishing

COMMUNICATION

View Article Online
View Journal | View Issue

A reversible fluorescent probe for detecting hypochloric acid in living cells and animals: utilizing a novel strategy for effectively modulating the fluorescence of selenide and selenoxide†

Cite this: *Chem. Commun.*, 2013, **49**, 2445

Received 29th December 2012,
Accepted 5th February 2013

DOI: 10.1039/c3cc39269d

www.rsc.org/chemcomm

Zhangrong Lou,[ab] Peng Li,[a] Qiang Pan[ab] and Keli Han*[a]

Based on a novel strategy for modulating the fluorescence of selenide and selenoxide, we have designed and developed a reversible fluorescent probe for hypochloric acid. And the synthesis, characterization, fluorescence properties, as well as the biological applications in living cells and animals, have all been described.

Hypochloric acid (HOCl) is one of the biologically important reactive oxygen species (ROS) and can be produced from hydrogen peroxide and chloride ions catalyzed by the heme enzyme myeloperoxidase (MPO) in living organisms.[1] Although HOCl is a major strong oxidant that functions as a microbicidal agent in living organisms and has a dominant role in the immune system,[2] it may also contribute to extensive oxidative stress and oxidative damage due to the destruction of nucleic acids, proteins, and lipids *via* both oxidation and chlorination reactions.[1,3] Increasing evidence shows that extensive oxidative stress and oxidative damage are associated with numerous diseases, such as neurodegeneration including Parkinson's disease and Alzheimer's disease,[4] inflammatory diseases,[5] atherosclerosis[6] and cancer.[7] Cells often have their own set of antioxidant defense systems to maintain redox equilibrium, where intracellular thiols play essential roles. For example, glutathione (GSH), which has been identified as the most abundant non-protein thiol, is considered to be the main player in combating oxidative stress and regulating the redox environment of the internal cellular compartments.[8] In addition, evidence has demonstrated that hydrogen sulfide (H_2S) functions as an effective HOCl scavenger to protect cells from oxidative stress.[9] And the complex redox biology of the cell governs many essential biological processes and has broad implications in human health and diseases.[10] In this regard, it is worth developing an effective technique to monitor the redox changes between HOCl and antioxidants in living systems.

Fluorescence imaging has the advantages of higher sensitivity, less invasiveness, and more convenience compared with other approaches, thereby providing more possibilities for the localization and dynamic monitoring of cellular metabolites.[11] Until now, even though several fluorescent probes for HOCl[12] have been reported, few reversible fluorescent probes for visualizing the redox changes mediated by HOCl and antioxidants have been developed.[13] Here we present such a reversible fluorescent probe for HOCl.

The reversible recognition moiety for an oxidation–reduction couple relies on the activity of glutathione peroxidase (GPx), which catalyzes the reaction between ROS and glutathione (GSH) *via* the oxidation–reduction cycles of the selenium center.[14] In addition, it is essential to introduce a fast excited state process to modulate the fluorescence of selenide and selenoxide. In our previous studies,[15] we have utilized photoinduced electron transfer (PET) and developed a reversible probe based on selenide and selenoxide successfully. In this study, we selected 1,8-naphthalimide as a signal transducer and designed a reversible fluorescent probe (NI–Se, Fig. 1a). The existence of the PET process in NI–Se has been denied by time-dependent density functional theory (TDDFT) calculations (ESI,† Fig. S1). However, the influences of viscosity and temperature experiments demonstrated that there was an excited state configuration twist process in NI–Se, but not in NI–SeO (Fig. S2, ESI†). And it is known that the excited state configuration twist always leads to fluorescence quenching.[16]

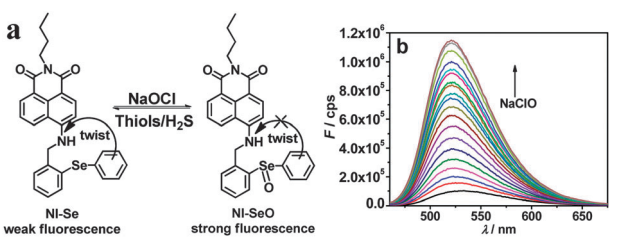

Fig. 1 (a) The structures of NI–Se and NI–SeO, and the proposed mechanism of fluorescence response to HOCl reversibly. (b) Changes in the fluorescence spectra of NI–Se with different concentrations of NaOCl.

[a] *State Key Laboratory of Molecular Reaction Dynamics, Dalian Institute of Chemical Physics (DICP), Chinese Academy of Sciences (CAS), 457 Zhongshan Road, Dalian 116023, P. R. China. E-mail: klhan@dicp.ac.cn; Fax: +86-411-84675584; Tel: +86-411-84379293*

[b] *Graduate School of Chinese Academy of Sciences, Beijing 100049, China*

† Electronic supplementary information (ESI) available: Additional fluorescent confocal images, fluorescence spectra assays, TDDFT calculations, details of the synthesis, ^{1}H NMR, ^{13}C NMR, ^{77}Se NMR, MS spectra of compounds discussed in this communication. See DOI: 10.1039/c3cc39269d

As a result, the fluorescence of NI–Se was enhanced in response to ROS. Here we also present the synthesis, characterization and fluorescence properties of this probe. And it turns out that this probe is highly sensitive, reversible and selective toward HOCl. Moreover, this probe is capable of visualizing HOCl and the reducing repair of living RAW 264.7 cells and living mice *in situ*.

The spectroscopic properties of NI–Se were measured under simulated physiological conditions (20 mM PBS, pH 7.40). Upon the addition of NaOCl as a HOCl source, an enhancement in fluorescence intensity was observed and the corresponding quantum yield of NI–Se increased from 0.04 to 0.45 (Fig. S3, ESI†). A fluorescence titration experiment demonstrated that fluorescent intensity increased linearly with the concentrations of NaOCl up to 15 μM (Fig. 1b, Fig. S4, ESI†). And the corresponding regression equation was F_{523nm} = 59 772 × [NaOCl] + 102 703 with a linear coefficient of r = 0.9941. In addition, the limit of detection for NaOCl was determined to be 5.86×10^{-7} M under the experimental conditions (ESI,† Fig. S5). No significant changes in the absorption intensity were observed with the increase in NaOCl concentrations (Fig. S4, ESI†).

The influence of pH on NI–Se both in the absence and presence of NaOCl was examined. Fig. S6 (ESI†) shows that NI–Se is stable in aqueous media from pH 4.0 to 12.0. Although a significant fluorescence decrease is observed over pH 9.0 in the presence of NaClO, NI–Se displays constant fluorescence intensity in the pH range of 4.0–9.0, demonstrating that NI–Se would work well under physiological pH conditions. The emission spectra of NI–Se with the addition of various ROS were investigated to evaluate the selectivity of NI–Se toward NaOCl screening compared to other biologically relevant species. As shown in Fig. 2a, a significant fluorescence response is observed for NaOCl, whereas a negligible fluorescence enhancement for other ROS. Additionally, the time courses of the probe with various ROS were recorded for 30 min to check whether the fluorescence switch might turn on upon incubation with other biological species over time (Fig. S7, ESI†). These results reveal that NI–Se is capable of responding to NaOCl *via* a turn-on fluorescence switch selectively over other ROS.

Having demonstrated that the probe can detect NaOCl selectively and stably over pH and time, we wonder whether NI–Se can respond to NaOCl reversibly in the presence of various reducing agents. As displayed in Fig. S8a (ESI†), no remarkable fluorescence intensity decrease is observed upon addition of reducing species and amino acids, except for H_2S and thiols. In addition, the fluorescence titration measurement of NI–SeO showed that the fluorescent intensity decreased gradually with increasing NaHS concentrations (Fig. S8b, ESI†). Next, the kinetics experiment of NI–Se response to NaOCl followed by H_2S was performed (Fig. 2b). The fluorescence intensity was stable over 1 h, suggesting that the probe solution was stable to light and air under the experimental conditions. And the emission intensity at 523 nm decreased significantly upon the addition of H_2S. When the solution was treated again with NaOCl, the fluorescence of the probe was recovered and the reversible oxidation–reduction cycles can be repeated six times with the fluorescence intensity decreased by about 50% (Fig. S8c, ESI†). The redox cycles have been confirmed through HPLC analyses (Fig. S9, ESI†). These experimental results revealed that NI–Se was capable of monitoring NaOCl reversibly in the presence of H_2S.

Subsequently, we applied NI–Se to imaging HOCl in living cells. The mouse macrophage cell line RAW264.7, which produced HOCl when stimulated by lipopolysaccharide (LPS) and phorbol myristate acetate (PMA), was chosen as the bioassay model.[12j] Fig. 3a shows that living RAW264.7 cells incubated with NI–Se exhibit only faint fluorescence. However, the cells that were pretreated with LPS and then incubated with PMA and NI–Se display green cellular fluorescence (Fig. 3b). Weaker cellular fluorescence is observed when the cells were pretreated with salicylhydroxamic acid (SHA), a MPO inhibitor[17] (Fig. 3c). Notably, co-staining with Hoechst 33342 (labels the nucleus) revealed that the probe located mainly in the cytoplasm of these living RAW264.7 cells (Fig. 3d).[18] And the relevant brightfield transmission images confirmed that the cells were still viable (ESI†). In addition, the MTT assay of the RAW264.7 cells with probe concentrations of 10.0 μM to 100.0 μM for 24 h demonstrated that NI–Se has low toxicity to cultured cell lines under the experimental conditions at a concentration of 10.0 μM (Fig. S10, ESI†). These results indicated that NI–Se was capable of monitoring HOCl in living RAW264.7 cells.

Since NI–Se is responsive to HOCl in living cells, we then investigated whether it could image the reducing repair of antioxidants. The living RAW264.7 cells loaded with NI–Se display only faint fluorescence (Fig. S13a, ESI†). However, treating the same NI–Se-incubated cells with PMA results in an increased cellular fluorescence intensity because of the generation of HClO

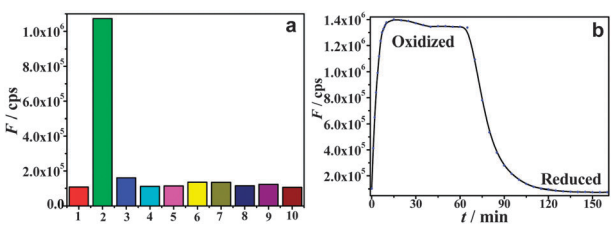

Fig. 2 (a) Fluorescence responses of NI–Se to various analytes. Bars represent the fluorescence intensity at 523 nm, responding to various ROS: 1, free; 2, NaOCl (30.0 μM); 3, peroxynitrite (300.0 μM); 4, NO (150 μM); 5, *tert*-butylhydroperoxide (300.0 μM); 6, cumene hydroperoxide (300.0 μM); 7, O_2^- (300.0 μM); 8, $^1O_2$ (300.0 μM); 9, H_2O_2 (300.0 μM); 10, •OH (300.0 μM). (b) Time course of NI–Se measured by a spectrofluorometer. NI–Se was oxidized by 5 equiv. of NaOCl for 1 h, and then treated with 20 equiv. of NaHS for 1.5 h.

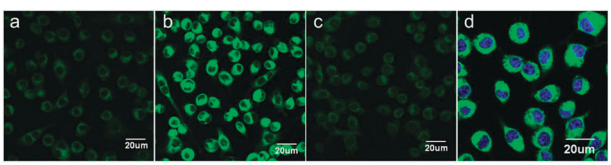

Fig. 3 Confocal fluorescence images of HOCl in living RAW264.7 cells. (a–c) RAW264.7 cells were pretreated with 1 μg mL^{-1} LPS for 16 h. (a) Incubated with 10 μM NI–Se for 5 min. (b) Incubated with 10 μM NI–Se for 5 min and then coincubated with 2.5 μg mL^{-1} PMA for 30 min. (c) Incubated with 10 mM SHA for 20 min and co-incubated with 2.5 μg mL^{-1} PMA for another 30 min, then incubated with 10 μM NI–Se. (d) RAW264.7 cells loaded with 2 μM Hoechst 33342 and 10 μM NI–Se for 5 min, Overlay of the NI–Se and Hoechst 33342 sets. NI–Se set (excitation: 488 nm, emission: 490–590 nm). Hoechst 33342 set (excitation: 405 nm, emission: 410–460 nm). Scale bar represents 20 μm.

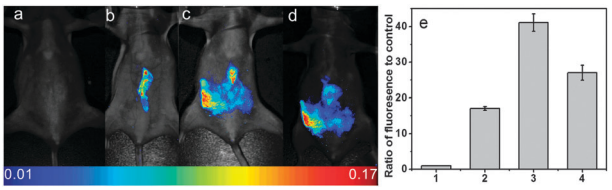

Fig. 4 Fluorescent images of HClO production and H_2S reduction in the peritoneal cavity of the mice with NI–Se. (a) Control, neither LPS nor NI–Se was injected; (b) saline was injected in the intraperitoneal (i.p.) cavity of mice, followed by i.p. injection of NI–Se (100 nmol); (c) LPS (1 mg) was injected into the peritoneal cavity of the mice, followed by i.p. injection of NI–Se (100 nmol). (d) An additional H_2S (4 μmol) was injected in parallel to (c). (e) (1)–(4) represent quantification of fluorescence emission intensity from (a)–(d), respectively. The total number of photons from the entire body of the groups (a)–(d) was integrated and plotted as a ratio to the control (a).

(Fig. S13b, ESI†). Decreased intracellular fluorescence is observed when the stimulated RAW264.7 cells were treated with the ROS scavenger[19] Glutathione S-Transferase (GST, EC: 2.5.1.18, 5 U mL^{-1}) (Fig. S13c, ESI†). The subsequent treatment of cells with PMA resulted in an increased cellular fluorescence (Fig. S13d, ESI†), demonstrating that the low levels of intracellular fluorescence in Fig. S13c (ESI†) were not due to photobleaching or dye leakage. In summary, these results suggested that NI–Se was capable of being developed as a fluorescence probe to image HOCl and the reducing repair in living cells.

Finally, NI–Se was applied to visualize HOCl and the reducing repair in living mice. The HClO was generated by activated macrophages and neutrophils in a lipopolysaccharide (LPS) model of acute inflammation.[12j,20] The untreated mouse was set as the control (Fig. 4a), and the mouse injected with both LPS and NI–Se (Fig. 4c) exhibited more fluorescence than that treated with NI–Se only (Fig. 4b). However, further injection of H_2S to the mouse parallel to (c) led to a decrease in fluorescence intensity (Fig. 4d). In addition, the fluorescent intensity from the entire body of the mice was quantified, and it can be noted that the mouse loaded with LPS and NI–Se exhibited higher fluorescence than the mouse loaded with saline and NI–Se. And lower fluorescence intensity was observed in the additional H_2S treated mouse (Fig. 4e). Taken together, NI–Se can be developed as a fluorescent probe for imaging HOCl and the reducing repair of antioxidants in living mice.

Mimicking the GPx centre and taking advantage of the mechanism of the twisting process, we have designed a reversible fluorescent probe for HOCl. The PET process has been excluded by TDDFT calculations, and the twisting process in NI–Se has been verified by the influences of viscosity and temperature experiments. (Further studies focusing on the driving force of the twist are currently underway). Here we also present the synthesis, characterization and fluorescence properties of this probe. And the fluorescent probe exhibits several advantages in terms of selectivity, sensitivity and reversibility. Importantly, combining the confocal fluorescence microscopy, this probe has been applied to visualize the HOCl and reducing repair of living cells and living mice *in situ*. Therefore, this study highlights a promising strategy for designing fluorescent probes, and provides a potential tool for further research in relevant biological processes of redox biology in living systems.

This work was supported by NSFC (no. 21273234 and 21203192) and the National Basic Research Program of China (2013CB834604). We are also grateful to Bingshuai Wang, Songqiu Yang, Ping Song for their contribution to the discussion of results. Thanks are also due to Jian Luo and Xiaohu He for critical reading of this article.

Notes and references

1 M. P. Curtis, A. J. Hicks and J. W. Neidigh, *Chem. Res. Toxicol.*, 2011, **24**, 418–428.
2 A. L. P. Chapman, M. B. Hampton, R. Senthilmohan, C. C. Winterbourn and A. J. Kettle, *J. Biol. Chem.*, 2002, **277**, 9757–9762.
3 (*a*) P. Nagy and M. T. Ashby, *J. Am. Chem. Soc.*, 2007, **129**, 14082–14091; (*b*) G. Drabik and J. W. Naskalski, *Acta Biochim. Pol.*, 2001, **48**, 271–275.
4 Y. W. Yap, M. Whiteman and N. S. Cheung, *Cell. Signalling*, 2007, **19**, 219–228.
5 Y. Maruyama, B. Lindholm and P. Stenvinkel, *J. Nephrol.*, 2004, **17**, S72–S76.
6 S. Sugiyama, K. Kugiyama, M. Aikawa, S. Nakamura, H. Ogawa and P. Libby, *Arterioscler., Thromb., Vasc. Biol.*, 2004, **24**, 1309–1314.
7 L. C. Adam and G. Gordon, *Anal. Chem.*, 1995, **67**, 535–540.
8 C. T. Dooley, T. M. Dore, G. T. Hanson, W. C. Jackson, S. J. Remington and R. Y. Tsien, *J. Biol. Chem.*, 2004, **279**, 22284–22293.
9 (*a*) B. Lee Predmore, D. Joseph Lefer and G. Gojon, *Antioxid. Redox Signaling*, 2012, **17**, 119–140; (*b*) M. Whiteman, N. S. Cheung, Y.-Z. Zhu, S. H. Chu, J. L. Siau, B. S. Wong, J. S. Armstrong and P. K. Moore, *Biochem. Biophys. Res. Commun.*, 2005, **326**, 794–798.
10 (*a*) E. W. Miller, S. X. Bian and C. J. Chang, *J. Am. Chem. Soc.*, 2007, **129**, 3458–3459; (*b*) Y. Koide, M. Kawaguchi, Y. Urano, K. Hanaoka, T. Komatsu, M. Abo, T. Teraia and T. Nagano, *Chem. Commun.*, 2012, **48**, 3091–3093; (*c*) B. C. Dickinson, J. Peltier, D. Stone, D. V. Schaffer and C. J. Chang, *Nat. Chem. Biol.*, 2011, **7**, 106–112.
11 Z. Lou, P. Li, X. Sun, S. Yang, B. Wang and K. Han, *Chem. Commun.*, 2013, **49**, 391–393.
12 (*a*) S. Kenmoku, Y. Urano, H. Kojima and T. Nagano, *J. Am. Chem. Soc.*, 2007, **129**, 7313–7318; (*b*) Y. Koide, Y. Urano, K. Hanaoka, T. Terai and T. Nagano, *J. Am. Chem. Soc.*, 2011, **133**, 5680–5682; (*c*) S. M. Chen, J. X. Lu, C. D. Sun and H. M. Ma, *Analyst*, 2010, **135**, 577–582; (*d*) G. Chen, F. Song, J. Wang, Z. Yang, S. Sun, J. Fan, X. Qiang, X. Wang, B. Dou and X. Peng, *Chem. Commun.*, 2012, **48**, 2949–2951; (*e*) X. Chen, K. A. Lee, E. M. Ha, K. M. Lee, Y. Y. Seo, H. K. Choi, H. N. Kim, M. J. Kim, C. S. Cho, S. Y. Lee, W. J. Lee and J. Yoon, *Chem. Commun.*, 2011, **47**, 4373–4375; (*f*) X. Q. Chen, X. C. Wang, S. J. Wang, W. Shi, K. Wang and H. M. Ma, *Chem.–Eur. J.*, 2008, **14**, 4719–4724; (*g*) J. Shepherd, S. A. Hilderbrand, P. Waterman, J. W. Heinecke, R. Weissleder and P. Libby, *Chem. Biol.*, 2007, **14**, 1221–1231; (*h*) W. Y. Lin, L. L. Long, B. B. Chen and W. Tan, *Chem.–Eur. J.*, 2009, **15**, 2305–2309; (*i*) L. Yuan, W. Lin, J. Song and Y. Yang, *Chem. Commun.*, 2011, **47**, 12691–12693; (*j*) L. Yuan, W. Lin, Y. Yang and H. Chen, *J. Am. Chem. Soc.*, 2012, **134**, 1200–1211; (*k*) Z.-N. Sun, F.-Q. Liu, Y. Chen, P. K. H. Tam and D. Yang, *Org. Lett.*, 2008, **10**, 2171–2174; (*l*) Y. K. Yang, H. J. Cho, J. Lee, I. Shin and J. Tae, *Org. Lett.*, 2009, **11**, 859–861; (*m*) X. D. Lou, Y. Zhang, Q. Q. Li, J. G. Qin and Z. Li, *Chem. Commun.*, 2011, **47**, 3189–3191.
13 B. Wang, P. Li, F. Yu, P. Song, X. Sun, S. Yang, Z. Lou and K. Han, *Chem. Commun.*, 2013, **49**, 1014–1016.
14 (*a*) K. P. Bhabak and G. Mugesh, *Acc. Chem. Res.*, 2010, **43**, 1408–1419; (*b*) G. Mugesh, W.-W. du Mont and H. Sies, *Chem. Rev.*, 2001, **101**, 2125–2180.
15 F. Yu, P. Li, G. Li, G. Zhao, T. Chu and K. Han, *J. Am. Chem. Soc.*, 2011, **133**, 11030–11033.
16 Q. Li, M. Peng, H. Li, C. Zhong, L. Zhang, X. Cheng, X. Peng, Q. Wang, J. Qin and Z. Li, *Org. Lett.*, 2012, **14**, 2094–2097.
17 Y. Adachi, A. L. Kindzelskii, A. R. Petty, J. B. Huang, N. Maeda, S. Yotsumoto, Y. Aratani, N. Ohno and H. R. Petty, *J. Immunol.*, 2006, **176**, 5033–5040.
18 M. E. Lalande, V. Ling and R. G. Miller, *Proc. Natl. Acad. Sci. U. S. A.*, 1981, **78**, 363–367.
19 F. Angelucci, P. Baiocco, M. Brunori, L. Gourlay, V. Morea and A. Bellelli, *Structure*, 2005, **13**, 1241–1246.
20 K. Kundu, S. F. Knight, N. Willett, S. Lee, W. R. Taylor and N. Murthy, *Angew. Chem., Int. Ed.*, 2009, **48**, 299–303.